

## Demonstration of Raman gain at 800 nm in single-mode fiber and its potential application to biological sensing and imaging

Keisuke Goda,<sup>a)</sup> Ata Mahjoubfar, and Bahram Jalali

Department of Electrical Engineering, University of California, Los Angeles, California 90095, USA

(Received 21 October 2009; accepted 25 November 2009; published online 21 December 2009)

Optical amplification prior to photon-to-electron conversion improves detection sensitivity in spectroscopic and imaging applications. Here we report the first experimental demonstration of Raman amplification in a single-mode fiber at wavelengths near 800 nm. This approach can potentially enable fast real-time optical sensing and imaging in the wavelength band that benefits from both low water absorption and the availability of high-power Ti:Sapphire lasers.

© 2009 American Institute of Physics. [doi:10.1063/1.3275739]

Fast real-time optical sensors are indispensable tools for pattern-recognition in applications including barcode reading, fingerprint matching, and face recognition, light detection and ranging, and industrial inspection and monitoring.<sup>1,2</sup> They are equally important for studying dynamic phenomena in biological and biochemical processes.<sup>3,4</sup> The central requirement for real-time operation is a signal integration time that is much shorter than the time scale of changes in the dynamic process. This requirement is very difficult to achieve because of the fundamental trade-off between sensitivity and speed; at high scan rates, fewer photons are collected during each integration time, leading to the loss of sensitivity.<sup>1–6</sup> One prominent example of applications that require high scan rates and high detection sensitivity is laser scanning fluorescence microscopy and two-photon microscopy used to observe neural activity in real time.<sup>7</sup>

In conventional high-speed detection, photodetectors [e.g., photodiodes and photomultiplier tubes (PMTs)] have to be cooled to reduce the thermal (electronic) noise level. However, cooling is undesirable as it requires a refrigeration unit to accompany the detector. Another technique used to increase the sensitivity is the use of a high-intensity illuminator. This approach is not suited for biological sensing as it can damage the sample especially in microscopy in which the light needs to be focused onto a very small field-of-view, resulting in extremely high optical power density (intensity). Optical amplification before the photon-to-electron conversion can overcome this fundamental challenge when the detection sensitivity is thermal noise limited. It eliminates the need for cooling and high-intensity illumination and therefore represents a powerful technique for detection of weak signals in spectroscopic and imaging applications.

This so-called optical preamplification is exploited heavily in long-haul fiber-optic communications<sup>8</sup> where the severely attenuated optical signal would otherwise be drowned in the thermal noise of the optoelectronic converter (i.e., the photodiode and subsequent electronic amplifier). Optical preamplification then improves the sensitivity of the receiver by raising the weak signal above the thermal noise floor. Unfortunately, rare-earth (e.g., erbium) doped fiber amplifiers, the workhorse of fiber-optic communications, are limited to operation in the 1550 nm wavelength range—a spectral region that is not suited for biological sensing be-

cause of the strong water absorption (three to four orders of magnitude stronger than at 800 nm). Semiconductor optical amplifiers (SOAs) can operate at other wavelengths; however, they suffer from high noise figures and hence are not well suited as preamplifiers.

Optical amplification is fundamentally different from electronic signal intensifiers (e.g., microchannel plates used in PMTs) in that amplification occurs in the optical domain whereas in microchannel plates, it occurs in the electronic domain. Electronic signal intensifiers are complex vacuum tube devices that require high voltage sources. Also, their scan rate is limited by the fundamental trade-off between gain and bandwidth in all electronic systems.<sup>9</sup>

The 800 nm band (700–900 nm) is important for biomedical applications because of the availability of the popular Ti:Sapphire lasers and also because it permits much larger penetration depths in tissue. The latter is due to a compromise between Rayleigh scattering (that increases at shorter wavelengths) and water absorption (that increases at longer wavelengths) in this wavelength band.<sup>10</sup> Compared to shorter wavelengths, the 800 nm band is also important for fluorescence microscopy with fluorescent dyes or quantum dots as background noise due to autofluorescence is greatly reduced.<sup>11</sup> The low absorptivity and scattering of light in tissue in this band enable *in vivo* imaging and subcellular sensing applications.

Compared to different approaches to optical amplification, stimulated Raman scattering (SRS) (Ref. 12) provides several advantage over other methods such as rare-earth doped fiber amplifiers and SOAs. First, gain is possible at any wavelength as long as a pump is available at a frequency blue-shifted from the signal by the optical-phonon vibrational frequency.<sup>12</sup> Second, a broad and flexible gain spectrum can be obtained by using multiple pumps.<sup>8,13</sup> Finally, Raman amplifiers have a lower noise figure than rare-earth doped fiber amplifiers and SOAs.<sup>8,13</sup> It is also ideal for amplified dispersive Fourier transformation<sup>5,6,14,15</sup>—a new technique that enables fast real-time spectroscopy and imaging.

In this letter, we report, to the best of our knowledge, the first experimental demonstration of Raman amplification in an optical fiber in the 800 nm band. Furthermore, we show the first measurement of the Raman gain coefficient near 800 nm. Because of limited pump power available and the large losses in the fiber used in these experiments, no net amplification could be achieved. However, we show that

<sup>a)</sup>Electronic mail: goda@ee.ucla.edu.

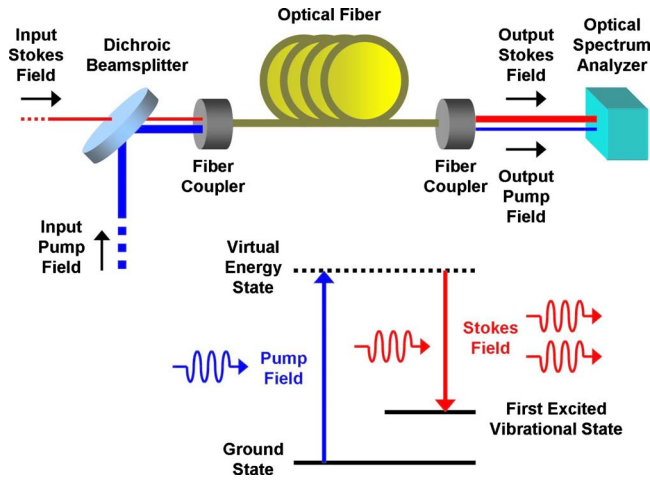


FIG. 1. (Color online) Distributed Raman amplification in an optical fiber. The input Stokes field is amplified by stimulated Raman scattering (SRS) in the fiber. The amplified Stokes field is detected by the optical spectrum analyzer.

with higher pump powers than what was available in our experiment and which are within the range of commercial amplified Ti:Sapphire lasers, significant net gain can be achieved.

Raman amplification is an optical process based on the phenomenon of SRS in which an input light (called the Stokes field) induces the inelastic scattering of a blue-shifted pump light in an optical medium (typically, an optical fiber) in the nonlinear regime.<sup>10</sup> As with rare-earth doped fiber amplifiers,<sup>7</sup> the process of Raman amplification is routinely employed as a low-noise optical amplifier in fiber-optic communications using transmission fibers as gain media.<sup>11</sup> SRS is described by the following coupled equations:<sup>10</sup>

$$\frac{dI_s}{dz} = g_R I_p I_s - \alpha_s I_s, \quad (1)$$

$$\frac{dI_p}{dz} = -\frac{\omega_p}{\omega_s} g_R I_s I_p - \alpha_p I_p, \quad (2)$$

where  $I_s$  and  $I_p$ , and  $\omega_s$  and  $\omega_p$  are the intensity and optical frequency of the Stokes and pump fields in the fiber, respectively,  $\alpha_s$  and  $\alpha_p$  are the loss coefficient of the fiber at the Stokes and pump frequencies, respectively,  $g_R$  is the Raman gain coefficient, and  $z$  is the propagation length. Assuming that the first term is much smaller than the second term on the right hand side in Eq. (2), Eqs. (1) and (2) can be solved for the Stokes intensity as a function of  $z$

$$I_s(z) = I_s(0) \exp \left\{ \frac{g_R}{\alpha_p} [(1 - e^{-\alpha_p z}) I_{p1}(0) + (e^{-\alpha_p(L-z)} - e^{-\alpha_p L}) I_{p2}(L)] \right\} \exp(-\alpha_s z) \quad (3)$$

where  $L$  is the total length of the fiber, and  $I_{p1}(0)$  and  $I_{p2}(L)$  are the forward (copropagating) and backward (counter-propagating) pump intensities at the injection points, respectively. This equation describes a general case of a dual (forward and backward) pumping architecture.

To demonstrate Raman amplification, we constructed the experiment (for forward pumping) shown in Fig. 1. A weak continuous-wave solid-state laser at 808 nm (CrystalLaser) is

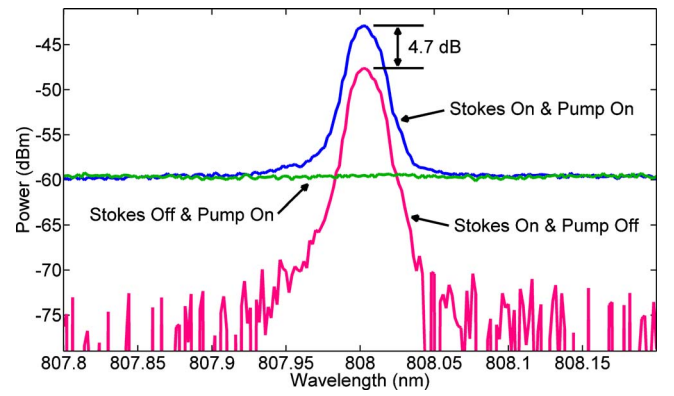


FIG. 2. (Color online) Experimental demonstration of Raman amplification at 808 nm in a single-mode fiber. The presence of the pump field amplified the Stokes field by 4.7 dB. The contribution of the fluorescence noise from the Ti:Sapphire crystal to the amplified Stokes field is negligible as the difference in power between them is more than 10 dB. The noise can be further reduced by backward pumping.

the amplifier input (Stokes field) that enters a 5 km long Ge-doped silica-core single-mode fiber with a mode-field diameter of 4  $\mu\text{m}$  (Nufern) via a fiber coupler. The small mode-field area increases the nonlinear interaction in the fiber. The fiber is forward-pumped by a continuous-wave frequency-tunable Ti:Sapphire laser at around 788 nm (KM Laboratories). The pump power coupled into the fiber is about 200 mW. The spectrum of the output Stokes field is measured with an optical spectrum analyzer.

Experimental results are shown in Fig. 2. First, the pump field was turned on and off to isolate the effect of Raman amplification. Then, with the pump on, the Stokes field was turned on and off to observe the noise level of the pump field. Finally, with the Stokes field off, we varied the pump power and observed the signal at the Stokes wavelength to observe any amplified spontaneous emission (ASE) arising from the SRS process. As shown in Fig. 2, any ASE was masked by the broadband fluorescence from the Ti:Sapphire crystal. The presence of the pump field in the fiber increased the Stokes power by 4.7 dB, indicating Raman amplification in the fiber. The contribution of the fluorescence from the Ti:Sapphire crystal to the amplified Stokes field is negligible as the difference in power between them is more than 10 dB. To validate Raman amplification in the fiber and exclude other possibilities, we measured the Stokes field before the fiber with and without the pump field and confirmed no difference in the Stokes field intensity between the two cases.

Furthermore, we also measured the Raman gain spectrum by tuning the pump wavelength for about 25 nm while keeping the Stokes wavelength fixed. Based on the measurements and Eq. (3), the Raman gain coefficient as a function of the frequency difference was deduced (Fig. 3) and is found to reach a value of  $5.4 \times 10^{-14}$  m/W at about 30 nm or 14 THz off-set from the pump (limited by the frequency tunable range of the Ti:Sapphire laser).

From independent measurements, the loss coefficients of the fiber,  $\alpha_s$  and  $\alpha_p$ , are found to be  $7.8 \times 10^{-4}$  m<sup>-1</sup> or  $-3.4$  dB/km (approximately equal for both). Based on these values and the peak value of the Raman gain coefficient, the net gain can be estimated as a function of the propagation length and pump power (Fig. 4). To minimize the impact of pump depletion and attenuation, we consider a dual pumping (forward and backward) architecture. The pump powers shown

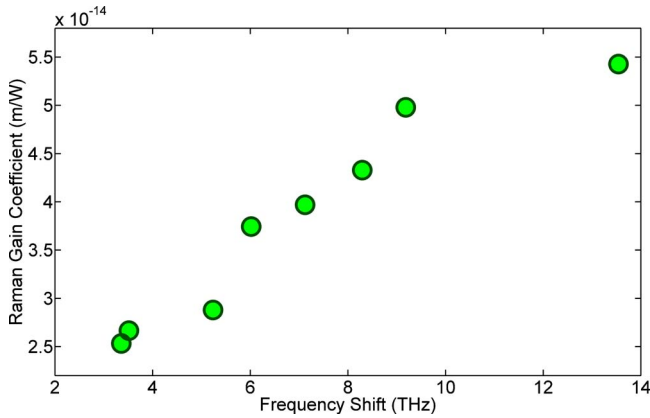


FIG. 3. (Color online) Measured Raman gain coefficient of the Ge-doped silica-core single-mode fiber at 808 nm as a function of the frequency difference between the Stokes and pump fields. We measured the Raman gain spectrum by tuning the pump wavelength for about 25 nm while keeping the Stokes wavelength fixed. Based on this data and Eq. (3), the Raman gain coefficient was deduced and used in our Raman amplifier model (Fig. 4).

in Fig. 4 are for each of the forward and backward pumps. The results indicate that if pump powers higher than 0.2 W achievable in our experiment are available, then net gain as high as 30 dB can be achieved. The 1 W pump level required for this is achievable with a commercially available amplified Ti:Sapphire laser.

One of the applications of Raman amplification in optical fibers is amplified dispersive Fourier transformation—an

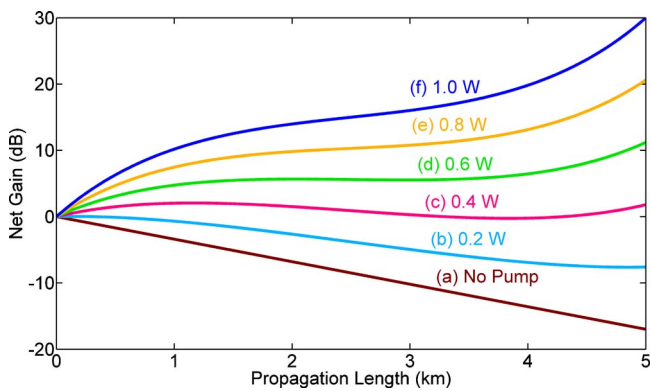


FIG. 4. (Color online) Net gain (gain minus fiber loss) as a function of the propagation length and pump power. A dual pumping (forward and backward) architecture is considered here. The pump powers shown in the figure are for each of the forward and backward pumps. While the maximum pump power available to us was 0.2 W, the model predicts that at a pump power level of 1 W (a value within the range of commercial amplified Ti:Sapphire lasers), a net gain of 30 dB may be possible.

optical process that maps the spectrum of an optical pulse into a temporal waveform using group-velocity dispersion (GVD) and amplifies it simultaneously.<sup>14,15</sup> Here, optical amplification is essential as it compensates for the loss in the GVD element and provides additional amplification to overcome the thermal (electronic) noise in the photodetector circuitry. This approach creates a spectrometer with internal optical gain and hence high sensitivity and high scan rates. Applications to ultrafast absorption<sup>16</sup> and Raman<sup>17</sup> spectroscopy and a new type of high-speed camera<sup>5</sup> have recently been demonstrated.

In conclusion, we have reported the first demonstration of Raman amplification in optical fibers at wavelengths near 800 nm—the scientifically and technologically important wavelength range. We have also measured the Raman gain coefficient. Optical amplification in this important wavelength range is expected to be valuable for high-speed and high-sensitivity optical sensing and imaging.

This work was supported by Defense Advanced Research Projects Agency (DARPA). We are grateful to our colleagues, especially K. K. Tsia and D. R. Solli, at UCLA Photonics Laboratory for discussions. We also thank J. Poon at Nufem and G. Taft at KM Laboratories.

<sup>1</sup>J. M. Lopez-Higuera, *Handbook of Optical Fibre Sensing Technology* (Wiley, New York, 2002).

<sup>2</sup>W. G. Rees, *Physical Principles of Remote Sensing* (Cambridge University Press, Cambridge, 2001).

<sup>3</sup>J. C. Mertz, *Introduction to Optical Microscopy*, 1st ed. (Roberts and Company, Greenwood Village, Colorado, 2009).

<sup>4</sup>A. Diaspro, *Confocal and Two-Photon Microscopy: Foundations, Applications and Advances*, 1st ed. (Wiley, Hoboken, New Jersey, 2001).

<sup>5</sup>K. Goda, K. K. Tsia, and B. Jalali, *Nature (London)* **458**, 1145 (2009).

<sup>6</sup>K. Goda, K. K. Tsia, and B. Jalali, *Appl. Phys. Lett.* **93**, 131109 (2008).

<sup>7</sup>P. Golshani, J. T. Goncalves, S. Khoshkhou, R. Mostany, S. Smirnakis, and C. Portera-Cailliau, *J. Neurosci.* **29**, 10890 (2009).

<sup>8</sup>G. P. Agrawal, *Fiber-Optic Communication Systems*, 3rd ed. (Wiley, New York, New York, 2002).

<sup>9</sup>P. Horowitz and W. Hill, *The Art of Electronics*, 2nd ed. (Cambridge University Press, Cambridge, U.K., 1989).

<sup>10</sup>J. G. Fujimoto, *Nat. Biotechnol.* **21**, 1361 (2003).

<sup>11</sup>H. W. Siesler, Y. Ozaki, S. Kawata, and H. M. Heise, *Near-Infrared Spectroscopy: Principles, Instruments, Applications*, 1st ed. (Wiley, Weinheim, Germany, 2002).

<sup>12</sup>G. P. Agrawal, *Nonlinear Fiber Optics*, 4th ed. (Academic, Burlington, Massachusetts, 2006).

<sup>13</sup>M. N. Islam, *IEEE J. Sel. Top. Quantum Electron.* **8**, 548 (2002).

<sup>14</sup>J. Chou, O. Boyraz, D. R. Solli, and B. Jalali, *Appl. Phys. Lett.* **91**, 161105 (2007).

<sup>15</sup>K. Goda, D. R. Solli, K. K. Tsia, and B. Jalali, *Phys. Rev. A* **80**, 043821 (2009).

<sup>16</sup>J. Chou, D. R. Solli, and B. Jalali, *Appl. Phys. Lett.* **92**, 111102 (2008).

<sup>17</sup>D. R. Solli, J. Chou, and B. Jalali, *Nat. Photonics* **2**, 48 (2008).